High Volumetric Energy Densities Capacitors Based on New Electrode Material Lanthanum Nitride

Wei-Bin Zhang [a], Xue-Jing Ma [a], Adeline Loh [b], Xiaohong Li [b], Frank C. Walsh [c], Ling-Bin Kong* [a]

[a] State Key Laboratory of Advanced Processing and Recycling of Non-Ferrous Metals, School of Materials Science and Engineering, Lanzhou University of Technology, Lanzhou 730050, China

[b] Renewable Energy Group, College of Engineering, Mathematics and Physical Sciences, University of Exeter, Penryn Campus, Cornwall TR10 9FE, UK

[c] Electrochemical Engineering Laboratory, Energy Technology Group, Faculty of Engineering and the Environment, University of Southampton, Southampton SO17 1BJ, UK

* Corresponding Author. E-mail: konglb@lut.cn

Abstract

LaN is synthesized via calcining La_2O_3 in NH_3 and studied as capacitive material for energy storage. A volumetric capacitance of 951.3 F cm^{-3} was found in 1 mol dm^{-3} Na_2SO_4 using a current density of 1 A g^{-1}, less than 1% loss of capacitance being experienced after 5000 cycles. 87.3% of the initial capacitance remained at a current density of 10 A g^{-1}. LaN exhibits high capacitances that is attributed to subsurface space charge accumulation with a possible EDLC component. A reversible electrode process ensures long cycle life and favourable electrical charge transfer. The assembled LaN symmetrical capacitor showed high volumetric energy densities, facilitating high duty applications.

Graphic Abstract

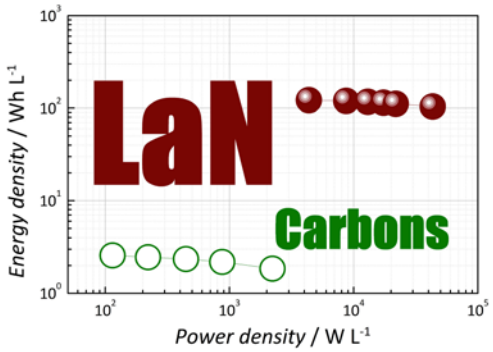

Activated carbons used in commercial electrode materials for capacitive energy storage exhibit a high specific capacitances.[1,2] However, their low bulk density makes them difficult to attain suitable volumetric properties,[3] thus alternative materials which possess high bulk density exceeding that of commercial activated carbon must be found.[4]

Several oxides have shown an impressive performance over the last decade,[5-9] but they tend to have a relatively low electrical conductivity.[10] This is a fatal flaw for electrode materials since the conductivity is directly related to electrochemical performance.[11] The carbons and the oxides respectively have their own advantages and fatal disadvantages. Materials, under the circumstances, with high bulk density and electrical conductivity are being required.

Most of intermetallics, a type of alloys, can exhibit high electrical conductivity and bulk density, which implies that they are candidates. As one of the intermetallics, LaN crystallizes in an NaCl-type lattice structure: the N atoms occupy octahedral interstices that form from the La atoms connected with metallic bonding and a theoretical bulk density of 6.73 g cm^{-3},[12] which suggest that it is an optional material. Its electrochemical capacitive performance in energy storage has not been developed and reported yet, even La-based materials either.

In this work, crystalline LaN nanoparticles possessing high specific area were synthesized via calcining of La_2O_3 in NH_3. The nanoparticles were electrochemically evaluated as a new electrode material in neutral aqueous electrolyte, which exhibits a promising capacitance that derives from subsurface space charge accumulation mechanism with a possible EDLC component. Furthermore, LaN-based symmetrical capacitor was cycled, showing good lifetime, energy density and specific capacitance.

LaN was synthesized via a one-step calcination method. Approximately 10 g La_2O_3 (Sinopharm® Chemical Reagent Co. Ltd.) powder was placed in a tube furnace under NH_3-N_2 (at a volume ratio of 8.5:1.5 and a flow rate of 70 mL min^{-1}) gas flow, heating at a rate of 3 °C min^{-1} from 20 °C; maintaining the temperature at 800 °C for 120 min, then cooling at 2 °C min^{-1} to a final temperature of 20 °C.

Materials chemical composition was analyzed by energy dispersive spectroscopy (EDS). Crystallite structures were determined via X-ray diffraction (XRD, Rigaku® D/MAX2400) with Cu K_α radiation (wave length 0.15418 nm) operating at 40 kV and 60 mA, the step is 0.02 and the speed is 1 deg min^{-1}. Structures and morphologies were characterized transmission electron microscope (TEM, JEOL® JEM2010) and field-emission scanning electron microscope (SEM, JEOL JSM-6701F) operating at 5.0 kV. Nitrogen adsorption-desorption (NAD) isotherms were obtained at -196 °C using a micromeritics gas adsorption analyzer (ASAPR® 2020). Before measurements, the sample (0.1 g) was degassed at 200 °C under vacuum for more than 2 h. The specific surface area was calculated according to the Brunauer-Emmett-Teller method.

For a 1 cm^2 electrode, 9.5 mg LaN and 0.5 mg PTFE were used as active material and binder respectively. These were mixed with a few drops of ethanol to achieve a composite gel. The gel was then cast as a film, which was pressed at 10

MPa into a stainless steel foam and then dried at 80 °C for 10 h.

A three-electrode glass cell with the LaN working electrode, a 1 cm^2 Pt foil counter electrode and a saturated calomel reference electrode (SCE) was used for electrochemical studies by using an electrochemical working station (Chenhua® CHI660C) in 1 mol dm^{-3} Na_2SO_4 (aq) at *ca.* 20 °C. Cyclic voltammetry (CV), galvanostatic charging-discharging (GCD) and electrochemical impedance spectroscopy (EIS) were used to evaluate the performance of electrode.

For a capacitor, two LaN electrodes were joined together by a porous non-woven cloth separator and soaked in the Na_2SO_4 (aq). The capacitor case is the stainless steel case used in lithium ion batteries (CR2032).

In addition, the electrical conductivity measurement is tested by tabletting resistance method and the LaN electrode for this test is prepared as follows. The LaN powders were tableted as a cylinder with the size of 78.5 mm^2 × 1mm by using the mould. And then, this cylinder electrode was directly used for electrical conductivity measurement using the electrochemical working station in air.

Figure 1a) shows the EDS spectra of the material obtained from the synthesis, which reveals that the material consist of La and N elements, the inherent Cu and C were not marked; only the La and N elements being present. It is inconclusive whether the material contains very little surface adsorbed oxygen. However, this material based electrode is tested in an aqueous solution in air environment. So, this result can be ignored if there is very little adsorbed oxygen.

Figure 1b) shows the XRD pattern of this material. As revealed in the pattern, diffraction peaks of LaN powder of (111), (200), (220), (311), (222), (400), and (331) are observed at diffraction angle of 29.159 deg, 33.796 deg, 48.545 deg, 57.636 deg,

60.456 deg, 71.090 deg, and 78.619 deg, respectively. The diffraction pattern is rigid in accordance with reported crystallographic data of cubic LaN (JCPDF No. 15-0892), and the space group is Fm $\bar{3}$m (225). In addition, the measured cubic cell parameter of 0.539 nm is very close to the standard value of 0.530 nm. There are no other peaks existing in the pattern. That is to say, there is no or scarcely any content of impurity. All the above reveals that the only LaN phase exists in the material. With the cell parameter, the crystallographic density calculated is *ca.* 6.68 g cm^{-3}. The calculated density is lower than the above-mentioned theoretical value, this is maybe due to some zero-dimensional atom point defects existed in the preparation of heat treatment. Chemical reaction that takes place during the material synthesis can be written:

$$La_2O_3 + 2NH_3 \xrightarrow{\Delta} 2LaN + 3H_2O\uparrow \quad (1)$$

Microstructure and morphology of the nanocrystalline LaN nanoparticles are shown in Figure 1c). Some nanoparticles are mutually interspersed, stabilizing the nanostructures and forming a three-dimensional structure. A granular appearance is implied in Figure 1d) since the quantity of heat that stored in chemical reactions (1) has to release along with thermal stress cracking during cooling to room temperature, and this process can produce the nanoparticles and build a porous structure.

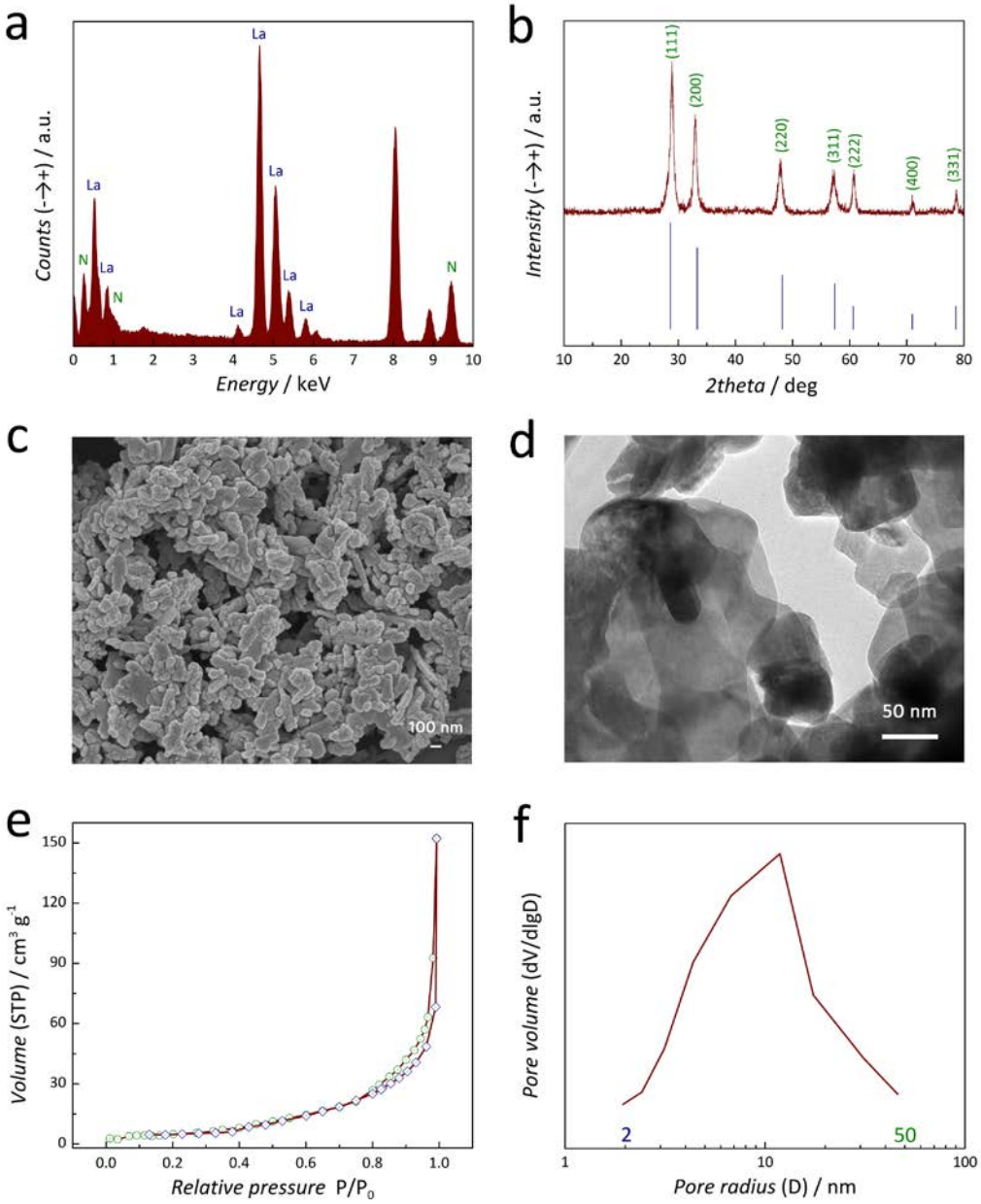

FIGURE 1. Materials and microstructural characterization. a) EDS spectrogram, b) XRD pattern, c) SEM image, d) TEM image, e) NAD data and f) Pore size distribution.

Figure 1e) shows NAD data of the nanoparticles. The existence of a hysteresis loop indicates a porous structure and the calculated specific surface area is 106.6 m^2 g^{-1}. Figure 1f) shows a pore size distribution estimated by a density function theory model.

Figure 2a) shows the CV curves of LaN electrode at a series of linear potential scan rates. Compared with carbon materials electrodes, a quasi-rectangular CV shape is achieved in the potential range from -0.9 to 0.6 V, which indicates typical capacitive charge storage behavior. Between 10 and 100 mV s^{-1}, quasi-rectangular CV shapes are similar to each other, i.e., the LaN electrode exhibited similar quasi-rectangular CV shapes at all scan rates, indicating reversible electrochemical charge storage and capacitive behavior.

GCD curves performed at some discrete current densities are shown in Figure 2b). The electrode showed more typical isosceles triangular shapes during consecutive charging and discharging, as expected for electrochemical capacitive charge storage. Based on the constant current discharge curves between 1 and 10 A g^{-1}, volumetric capacitances at certain current density are calculated via:

$$C_{\mathrm{v}} = \frac{\rho \cdot j_{\mathrm{i}} \cdot \Delta t}{\Delta \varphi} \tag{2}$$

where C_{v} (F cm^{-3}) is the volumetric capacitance, ρ (g cm^{-3}) is the density of LaN, j_{i} (A g^{-1}) is the specific current density, Δt (s) is discharging time and $\Delta \varphi$ (V) is the potential difference during discharge.

The results calculated from equation (2) and some carbon-based materials[13] are shown in Figure 2c). The volumetric capacitances of 951.3, 934.2, 916.9, 894.0, 871.1, and 830.9 F cm^{-3} correspond to a discharge current density of 1, 2, 3, 4, 5, and 10 A g^{-1}, respectively. And the corresponding mass specific capacitances are 143.7, 141.1, 138.5, 135.0, 131.6, and 125.5 F g^{-1}. These volumetric capacitances data are much higher than that of carbon-based materials at a current density of 1 A g^{-1}. Moreover, the LaN electrode also exhibited a high capacitance at this current density range. Even

at a high current density of 10 A g^{-1}, high capacitance value of 830.9 F cm^{-3} remains, which is almost 87.3% of the initial value for the current density from 1 A g^{-1} enlarging to 10 A g^{-1} or 10 times increasing.

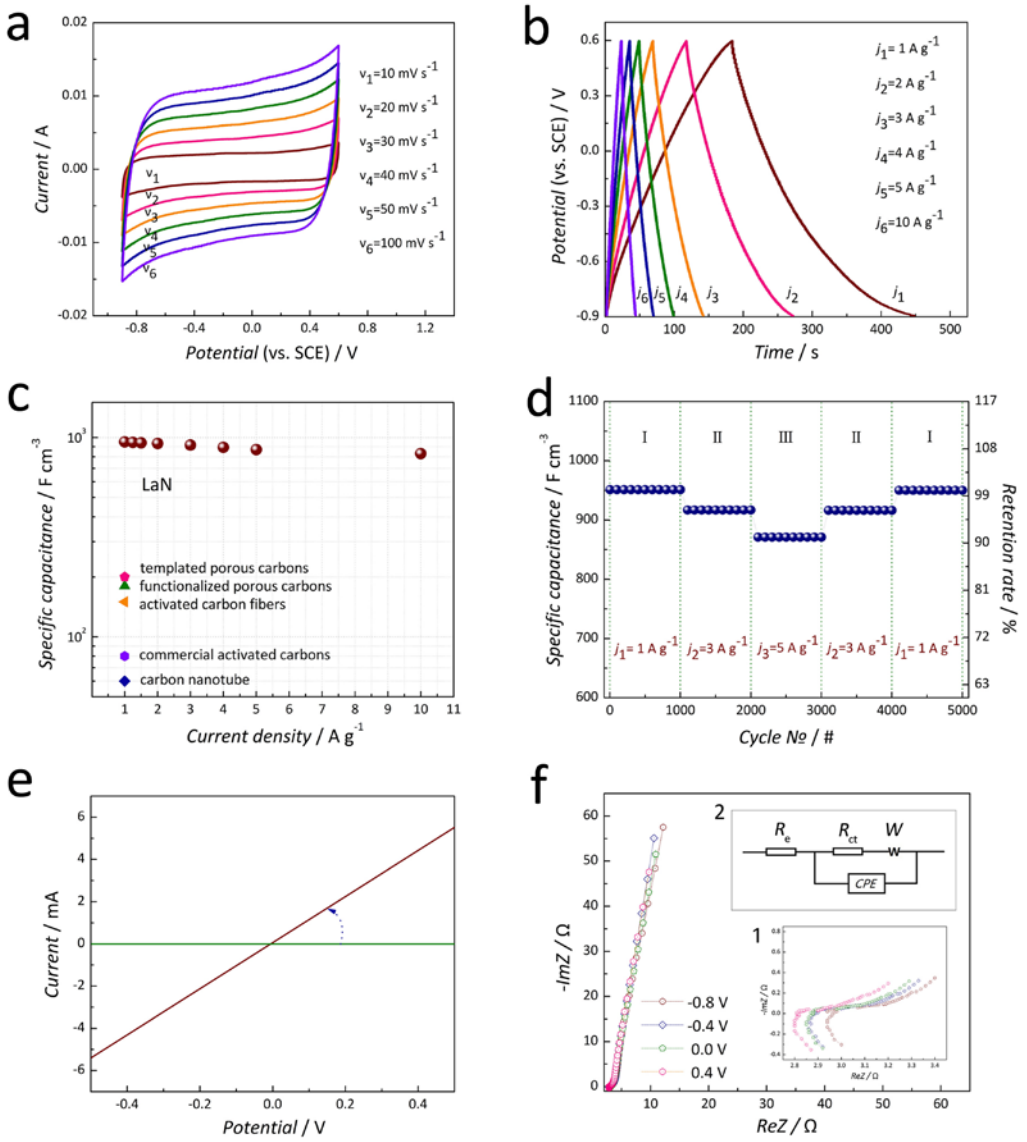

FIGURE 2. Electrochemical evaluation of the LaN. a) CV curves, b) GCD curves, c) Volumetric capacitance compared with some carbon-based materials, d) Cycle life over 5000 cycles, e) Current-voltage curves of the LaN and f) Electrochemical impedance spectroscopy.

In a general way, carbon materials possess volumetric capacitances ca. 60~125 F cm^{-3}.[4,13] The capacitance values of this novel material are calculated to be 7 to 9.5 times greater than that of carbon materials. In addition, rate capability compared to almost all of pseudocapacitive oxides is superb since the oxides always own a rate capability of 60~70%[14,15] or even less. All of above show an underlying application of this new material in some certain fields, especially in the areas that require volumetric property.

Based on the quasi-rectangular CVs and isosceles triangle GCDs, it seems that energy storage mechanism is much more likely to be EDLCs type. However, if we calculate the capacitance at per unit area, the result is in the range of 1.334 to 1.235 mF cm^{-2}, which is far beyond the established range (*ca.* 10^{-2} mF cm^{-2}) of EDLCs,[4,16] and there are no substantiated redox reactions, implying another mechanism existing in, but this conclusion does not exclude the inexistence of EDLCs. It is well known that pseudocapacitive reactions always give redox peaks and some of them can get rectangular CVs when possessing multiple overlapping reactions. Here, pianissimo peaks that are existed in the CVs are difficult to support the (leading) component of pseudocapacitance. While it reveals the existence of an anomalous new possible storage mechanism that non-faradic contribution and no redox reaction are involved, and was reported recently by Oleksandr Bondarchuk et al.[14] in a vanadium nitride electrode. That is an anomalous non-faradaic subsurface space charge accumulation mechanism. There is an active subsurface layer with a charge-accumulating effective thickness of up to dozens of nanometers. Here, another new material that owns this mechanism is found, and at the same time the result also underlines the Oleksandr Bondarchuk' work about finding this new mechanism during charging-discharging. So, based on capacitance, surface area calculation and other arguments mentioned above,

the main charge storage for this material is subsurface space charge accumulation mechanism with a possible minor EDLC component.

Figure 2d) depicts the cycle life of the LaN electrode. By step charging and discharging from zone I, II, III, II, and I, less than 1% initial capacitance is lost. The LaN electrode exhibits an excellent cycle life after 5000 cycles of unsteady charging and discharging.

The lifetime is another description of electrode reaction reversibility. In CV curves, the reversibility of the electrode reaction is closely related to (a) charge and (b) mass transfer. It is necessary to determine whether the electrode reaction is controlled by charge transfer or diffusion.

For instance, taking the average values of anodic peaks J_{pa} at various current densities, a linear relationship can be found by fitting the data with a least squares method.

$$\left[{}^{i}J_{pa}\right] \propto \left[\nu_{i}^{\frac{1}{2}}\right], \text{(i=1, 2, 3, 4, 5, 6).} \tag{3}$$

From this, we can determine that the electrode reaction is diffusion-controlled.

Similarly, taking the average values of cathode peaks J_{pc} and comparing with the average values of the anodic peaks $J_{pa,}$ the following formula is established.

$$\left[{}^{i}J_{pa}\right] = -\left[{}^{i}J_{pc}\right], \text{(i=1, 2, 3, 4, 5, 6).} \tag{4}$$

This expression is a sufficient criterion for high electrode reversibility under diffusion control factor (b), which we suggest has a positive impact on the electrode's cycle life.

Electrical conductivity is another important factor that influences the

electrochemical performance; materials with high conductivity provide sufficient electrons for fast surface redox reactions, ensuring good rate capability. Figure 2e) shows the current-voltage curves of the LaN tested by using linear sweep voltammetry. The calculated conductivity of LaN through the law of resistance is 0.34 S cm^{-1}, which is three to five orders of magnitude higher than capacitive oxides that typically show a conductivity of 10^{-6} to 10^{-4} S cm^{-1}.[10] The high electrical conductivity leads to a good rate capacity.

EIS during charging or discharging describes electric charges transfer resistance R_{ct} in some certain potential. Figure 2f) shows Nyquist plots of the LaN electrode in frequency range between 10^{-1}~10^{5} Hz operating at different potentials (-0.8 V, -0.4 V, 0 V and 0.4 V) and the amplitude is 0.005 V. The inset 1 shows the semicircle evident at high-frequency. Their impedance values for the different components were calculated via *ZSimpWin* software. The equivalent circuit used to fit the spectroscopy curve is also given in the inset 2. Because the LaN electrode reveals a capacitive behavior during charging-discharging with only one time constant existing. In this case, there are two types of equivalent circuit, i.e., the equivalent circuit with diffusive resistance (*W*) component or not. The electrode reaction is diffusion-controlled, so the equivalent circuit contains a diffusive *W* component. The R_e values of these curves calculated using the *ZSimpWin* are 3, 2.92, 2.92 and 2.87 Ω, respectively. And the calculated R_{ct} values are all ca. 0.02 Ω, showing a low resistance to electric charge transfer and a relatively good stability.

A symmetric capacitor was assembled using two identical prepared LaN electrodes and tested for investigating the usability. Figure 3a) shows GCD curves of the symmetric capacitor. According to formula (2), the capacitances are 390.9, 383.3, 375.2, 366.6, 356.7, and 335.8 F cm^{-3} correspond to a discharge current density of 1, 2,

3, 4, 5, and 10 A g^{-1}, respectively. Figure 3b) shows the Ragone plots of this capacitor, activated carbon capacitor and some reported capacitors[17] at their optimal conditions. Volumetric energy density E_v and power density P_v are calculated as:

$$E_v = \frac{1}{2} C_v \cdot U^2 \tag{5}$$

$$P_v = \frac{E_v}{\Delta t} \tag{6}$$

The LaN symmetric capacitor shows a superior volumetric energy density coupled with a high coulombic efficiency in Figure 3c) and a high thermal shock resistance in Figure 3d), indicating the potential value of LaN as a high performance capacitor material.

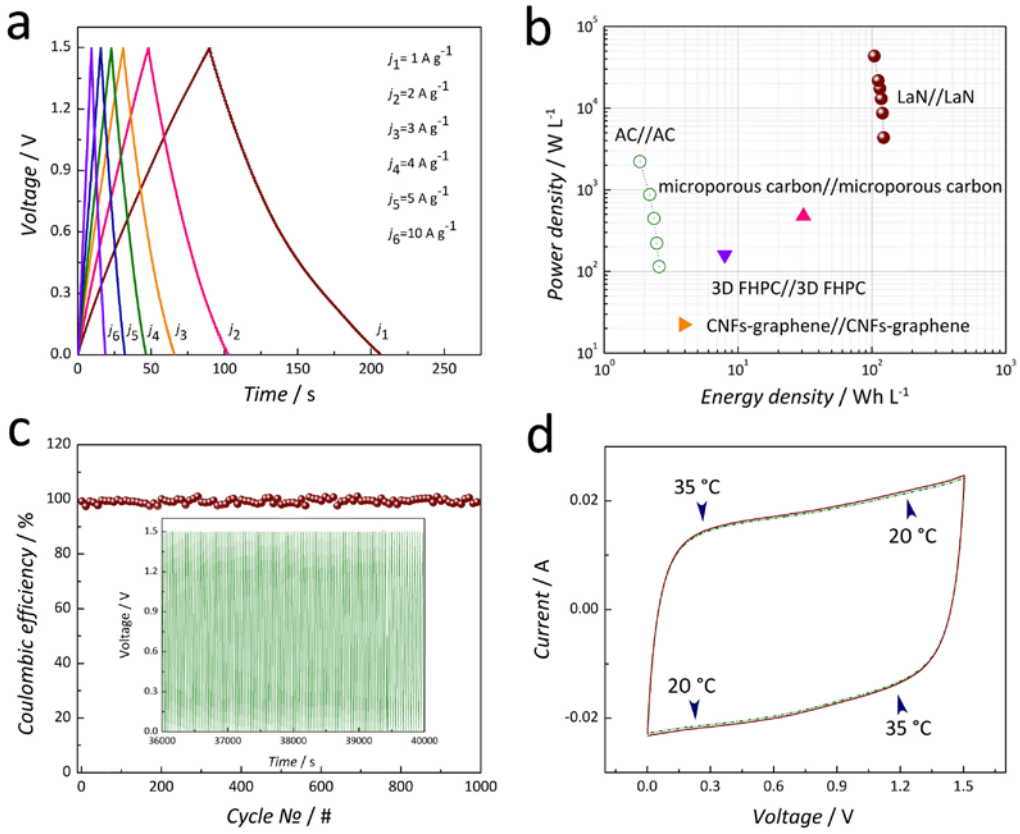

FIGURE 3. Electrochemical evaluation of the LaN symmetrical capacitor. a) GCD curves, b) Ragone plots of volumetric energy density *vs.* power density, c) Coulomb efficiency and d) Thermal shock resistance tested between 20 and 35 °C.

A new capacitive material has been synthesized and found for energy storage. A high volumetric capacitance of 951.3 F cm^{-3} is achieved at 1 A g^{-1} with less than 1% loss after 5000 cycles. This volumetric capacitance value is 7 to 9.5 times higher than activated carbons. The capacitance gives credit to subsurface space charge accumulation mechanism with a possible EDLC component. A highly reversible electrode reaction that controlled by diffusion and a high, stable electronic conductivity during charging or discharging ensure a long cycle life and electrical charge transfer rate. The LaN//LaN capacitor shows very high volumetric energy densities, which is hope for some volumetric requirement occasions. Further studies will endeavour to elucidate the exact charge storage mechanism in this material.

Acknowledgments

This work was financially supported by the National Natural Science Foundation of China (No.51362018) and the Foundation for Innovation Groups of Basic Research in Gansu Province (No.1606RJIA322).

References

(1) Goubard-Bretesché, N.; Crosnier, O.; Payen, C.; Favier, F.; Brousse, T. Nanocrystalline $FeWO_4$ as a Pseudocapacitive Electrode Material for High Volumetric Energy Density Supercapacitors Operated in an Aqueous Electrolyte. *Electrochem. Comm.* **2015**, *57*, 61-64.

(2) Li, Y. T.; Pi, Y. T.; Lu, L. M.; Xu, S. H.; Ren, T. Z. Hierarchical Porous Active

Carbon from Fallen Leaves by Synergy of K_2CO_3 and Their Supercapacitor Performance. *J. Power Sources* **2015**, *299*, 519-528.

(3) Laheäär, A.; Delpeux-Ouldriane, S.; Lust, E.; Béguin, F. Ammonia Treatment of Activated Carbon Powders for Supercapacitor Electrode Application. *J. Electrochem. Soc.* **2014**, 161, A568-A575.

(4) Porto, R. L.; Frappier, R.; Ducros, J. B.; Aucher, C.; Mosqueda, H.; Chenu, S.; Chavillon, B.; Tessier, F.; Cheviré, F.; Brousse, T. Titanium and Vanadium Oxynitride Powders as Pseudo-capacitive Materials for Electrochemical Capacitors. *Electrochim. Acta* **2012**, *82*, 257-262.

(5) Bissett, M. A.; Worrall, S. D.; Kinloch, I. A.; Dryfe, R. A. W. Comparison of Two-Dimensional Transition Metal Dichalcogenides for Electrochemical Supercapacitors. *Electrochim. Acta* **2016**, *201*, 30-37.

(6) Mendoza-Sánchez, B.; Brousse, T.; Ramirez-Castro, C.; Nicolosi, V.; Grant, P. S. An Investigation of Nanostructured Thin Film α-MoO_3 Based Supercapacitor Electrodes in an Aqueous Electrolyte. *Electrochim. Acta* **2013**, *91*, 253-260.

(7) Zhang, W. B.; Kong, L. B.; Ma, X. J.; Luo, Y. C.; Kang, L. Design, Synthesis and Evaluation of Three-dimensional $Co_3O_4/Co_3(VO_4)_2$ Hybrid Nanorods on Nickel Foam as Self-supported Electrodes for Asymmetric Supercapacitors. *J. Power Sources* **2014**, *269*, 61-68.

(8) Zolfaghari, A.; Ataherian, F.; Ghaemi, M.; Gholami, A. Capacitive Behavior of Nanostructured MnO_2 Prepared by Sonochemistry Method. *Electrochim. Acta* **2007**, *52*, 2806-2814.

(9) Rajeswari, J.; Kishore, P. S.; Viswanathan, B.; Varadarajan, T. K. One-dimensional MoO_2 Nanorods for Supercapacitor Applications. *Electrochem. Commun.* **2009**, *11*, 572-575.

(10) Zhi, M. J.; Xiang, C. C.; Li, J. T.; Li, M.; Wu, N. Q. Nanostructured Carbon-metal Oxide Composite Electrodes for Supercapacitors: a Review. *Nanoscale* **2013**, *5*, 72-88.

(11) Pico, F.; Ibañez, J.; Lillo-Rodenas, M. A.; Linares-Solano, A.; Rojas, R. M.; Amarilla, J. M.; Rojo, J. M. Understanding $RuO_2 \cdot xH_2O$/carbon Nanofibre Composites as Supercapacitor Electrodes. *J. Power Sources* **2008**, *176*, 417-425.

(12) Lanthanum Nitride. http://www.basechem.org/chemical/15793.

(13) Zhang, L. L.; Zhao, X. S. Carbon-based Materials as Supercapacitor Electrodes. *Chem. Soc. Rev.* **2009**, *38*, 2520-2531.

(14) Li, J.; Que, T. L.; Huang, J. B. Synthesis and Characterization of a Novel Tube-in-tube Nanostructured PPy/MnO_2/CNTs Composite for Supercapacitor. *Mater. Res. Bull.* **2013**, *48*, 747-751.

(15) Jiang, H.; Yang, L. P.; Li, C. Z.; Yan, C. Y.; Lee, P. S.; Ma, J. High-rate Electrochemical Capacitors From Highly Graphitic Carbon-tipped Manganese Oxide/mesoporous Carbon/manganese Oxide Hybrid Nanowires. *Energy Environ. Sci.* **2011**, *4*, 1813-1819.

(16) Bondarchuk, O.; Morel, A.; Bélanger, D.; Goikolea, E.; Brousse, T.; Mysyk, R. Thin Films of Pure Vanadium Nitride: Evidence for Anomalous Non-faradaic Capacitance. *J. Power Sources* **2016**, *324*, 439-446.

(17) Zhong, C.; Deng, Y. D.; Hu, W. B.; Qiao, J. L.; Zhang, L.; Zhang, J. J. A Review of Electrolyte Materials and Compositions for Electrochemical Supercapacitors. *Chem. Soc. Rev.* **2015**, *44*, 7484-7539.